Energy 44 (2012) 1017–1027

Contents lists available at SciVerse ScienceDirect

Energy

journal homepage: www.elsevier.com/locate/energy

Efficiencies of power flash cycles

Ngoc Anh Lai [a], Johann Fischer [b,*]

[a] Heat Engineering Department, Institute of Heat Engineering and Refrigeration, Hanoi University of Science and Technology, Hanoi, Viet Nam
[b] Institut für Verfahrens- und Energietechnik, Universität für Bodenkultur, Muthgasse 107, A-1190 Wien, Austria

ARTICLE INFO

Article history:
Received 30 January 2012
Received in revised form
12 April 2012
Accepted 20 April 2012
Available online 30 May 2012

Keywords:
Heat to power conversion
Trilateral cycle
Organic Rankine cycle
Organic working fluids
Process optimization
Exergy analysis

ABSTRACT

Power flash cycles (PFC) are a generalization of trilateral cycles (TLC) in which the compressed liquid is heated up to its boiling point and then performs a flash expansion during which it delivers power. The end point of the expansion may be in the wet vapour region (TLC) or in the dry vapour region. Here model results are presented for PFC-systems including the heat transfer to and from the cycles with aromates, siloxanes, and alkanes as working fluids. Optimization criterion is the exergy efficiency for power production at different pairs of heat carrier and cooling agent inlet temperatures ranging from (350 °C, 62 °C) to (150 °C, 15 °C). Comparisons with TLC for water, organic Rankine cycles (ORC) and water Clausius-Rankine cycles are made. General findings are that PFC has higher power production efficiencies than ORC but larger volume flows at the expander outlet. Moreover, TLC with water have in all cases the highest or nearly highest power production efficiencies. The disadvantage of water are the large outlet volume flows at low temperatures. For these cases alkanes like cyclopentane are to be preferred in PFC which can have significantly smaller outlet volume flows and rather high power production efficiencies.

1. Introduction

For conversion of low and medium temperature heat to power one can consider besides organic Rankine cycles (ORC) and Kalina cycles also trilateral cycles (TLC) and their generalizations which we call power flash cycles (PFC). In PFC the compressed liquid is heated up at constant pressure to its boiling point and then performs a flash expansion during which it delivers power. If the end point of the expansion is in the wet vapour region the process is represented in the temperature vs entropy (*T,s*)- diagram approximately by a triangle and hence this power flash cycle is called trilateral cycle. Depending on the working fluid and the process the end point of the expansion, however, may also lie in the dry vapour region and then the process resembles more to a quadrangle in the *T,s*-diagram. Whilst the latter process is sometimes also called TLC we call it quadrilateral cycle (QLC) and both cyles, TLC and QLC, are summarized as PFC.

There exists a wealth of literature on ORC [1–31] and on Kalina cycles [29–37]; in view of the large number of publications about these cycles the references given are by far not complete. Whilst ORC and Kalina cycles are used already in existing power plants, the PFC [38–53] are still in a state of technical development [46–48,50,52]. For an assessment of their efficiency we consider systems which include the heat transfer from the heat carrier to the working fluid, the cycle process, and the heat transfer from the working fluid to the cooling agent. In case that the heat carrier is a substance which cools down during the heat transfer the PFC has the advantage that the cooling down curve of the heat carrier and the heating up curve of the working fluid match well together which means a very efficient heat transfer and causes high system efficiency.

In a previous paper [53] a comparison was made between TLC with water as working fluid and ORC with optimal selected working fluids. Five cases specified by the heat carrier inlet temperature T_5 and the cooling agent inlet temperature T_7 were considered. The inlet temperature pairs range from (350 °C, 62 °C) for case I to (150 °C, 15 °C) for case *V*. The objective function for optimization was the exergy efficiency for power production ξ_P which is the ratio of the net power output to the incoming exergy flow of the heat carrier. The ORC working fluids considered are - depending on T_5 - cyclopentane, n-butane, and propane and optimal results were obtained with slightly sub- or supercritical pressures. We found that ξ_P is higher for the TLC-systems than for the ORC-systems for all temperature intervals. For the high temperature interval (280 °C, 62 °C) ξ_P is higher by 14% and for the lowest temperature interval (150 °C, 15 °C) by 29%. Besides the exergy efficiency ξ_P the second most interesting quantity is the volume flow $\dot{V}_4$ at the outlet of the expander which is important for the design of the expander and

* Corresponding author. Tel.: +43 1 3709726 201; fax: +43 1 3709726 210.
E-mail address: johann.fischer@boku.ac.at (J. Fischer).

0360-5442/$ – see front matter © 2012 Elsevier Ltd. All rights reserved.
doi:10.1016/j.energy.2012.04.046

Nomenclature

CRC	Clausius-Rankine cycle with superheating
$\dot{C}$	Heat capacity flow rate [kW/K]
c_p	Isobaric heat capacity [kJ/kgK]
e	Specific exergy [kJ/kg]
$\dot{E}$	Exergy flow rate [kW]
h	Specific enthalpy [kJ/kg]
IHE	Internal heat exchanger
$\dot{m}$	Mass flow rate [kg/s]
ORC	Organic Rankine cycle
ORCo2+	ORC at subcritical p_{max} without superheating with IHE
ORCs2+	ORC at supercritical p_{max} with IHE
ORCs2-	ORC at supercritical p_{max} without IHE
p	Pressure [MPa]
PFC	Power flash cycle
q	Specific heat [kJ/kg]
$\dot{Q}$	Heat flow rate [kW]
QLC	Quadrilateral cycle
QLC+	Quadrilateral cycle with IHE
QLC−	Quadrilateral cycle without IHE
s	Specific entropy [kJ/kgK] or [J/molK]
T	Temperature [K] or [°C]
TLC	Trilateral cycle
v	Specific volume [l/kg]
$\dot{V}$	Volume flow rate [l/s]
w	Specific work [kJ/kg]
$\lvert\dot{W}\rvert$	Net power output of a cycle [kW]

Greek symbols

Δ	Difference of quantities
$\eta_{s,P}$	Isentropic pump efficiency
$\eta_{s,E}$	Isentropic expander efficiency
η_{th}	Thermal efficiency of the cycle
ξ	Total exergy efficiency
ξ_P	Exergy efficiency for power production

Subscripts

1,2,3,4	State points of working fluid
2a, 4a	State points of working fluid in cycle with IHE
5,6	State points of heat carrier
7,8	State points of cooling agent
c	Critical point
CA	Cooling agent
E	Expander
HC	Heat carrier
i	State point
ij	Process from state point i to j
in	Ingoing flow
out	Outgoing flow
P	Pump, Power
p	Pinch (hot stream), isobaric
s	Isentropic
u	Environment state
WF	Working fluid

also for the sizing of the heat exchangers. The TLC with water have, however, the drawback that at low working fluid temperatures the volume flows become very large because of the low water vapour pressures.

Here we consider pure organic substances as working fluids for PFC with two aims. First, we expect that for low heat carrier inlet temperatures T_5 organic fluids with lower critical temperatures should lead to smaller volume flows $\dot{V}_4$ at the outlet of the expander. Second, we want to see whether organic fluids with high critical temperatures are better than water for high values of T_5. Thereto the same five cases as in [53] are studied. Comparison of the results for the PFC-systems with organic working fluids will be made with the TLC results for water and the optimal ORC results [53]. Moreover, we give also results for water Clausius–Rankine cycles (CRC) [54,55].

For the PFC-systems several classes of organic working fluids are examined. For the highest temperature interval we consider the aromates butylbenzene, ethylbenzene, m-xylene, and toluene and the linear siloxanes dodecamethylpentasiloxane (MD3M), decamethyltetrasiloxane (MD2M), octamethyltrisiloxane (MDM), and hexamethyldisiloxane (MM). Going to lower temperature intervals we remove successively the larger aromates and siloxanes and include the alkanes cyclopentane, n-pentane, isopentane, neopentane, and n-butane as well as the refrigerant R245ca. We remind that the vapour - liquid - equilibrium (VLE) curve in the temperature vs entropy (T,s)- diagram is bell-shaped for water but it may be strongly overhanging for organic fluids [8,22]. As this shape plays a significant role for the power flash cycles we will first consider this behaviour and its reason here in more detail.

The paper is organized such that in Section 2 the skewness of the VLE curves in the T,s-diagram is quantified. In Section 3 the configuration of the PFC-system and different types of cycles in the T,s-diagram are described. In Section 4 the thermodynamics of PFC is outlined including the process quantities, the heat transfers to and from the cycle as well as energy and exergy equations. In Section 5 we give results for the PFC-systems with organic working fluids, compare them with other heat to power conversion engines and discuss the findings. The paper is finished in Section 6 with a summary and conclusions.

2. Shape of VLE curves in the T,s-diagram

In most heat to power conversion engines as well as in most refrigeration machines and heat pumps the shape of the VLE curve in the T,s-diagram plays a significant role. The VLE curve in the T,s-diagram may either be bell (b)- shaped or overhanging (o) and correspondingly we speak about b- or o-fluids [8]. Evidently, these shapes are caused by the degree in which the entropy changes with increasing temperature. This item was already addressed in [56] and in [41] it was claimed that this increase is related to the number of atoms in a molecule. A physically more profound explanation is to relate this shape to the change of the ideal gas entropy which is mainly determined by the activated internal degrees of freedom in a molecule as e.g. vibrations and librations. In particular it was shown in [22] for the o-fluids cyclopentane, toluene, and MM that the VLE curve in the T,s-diagram becomes more skewed with increasing c_p^0.

Because of the practical importance of the skewness of the VLE curve in the T,s-diagram of o-fluids it may be useful to introduce a quantitative measure for it. From [41] and [22] it is known that for o-fluids the entropy on the dew line has a maximum value s''_{max} at a temperature $T(s''_{max})$ close to the critical temperature. At lower temperatures the entropy on the dew line decreases and may eventually pass through a minimum s''_{min} at a temperature $T(s''_{min})$. The interesting quantity is the average slope of the dew line between s''_{max} and s''_{min}. For cases where s''_{min} is not or not easily available as for the siloxanes one may take equally well the lowest

available entropy on the dew line which in these cases is generally close to a straight line. As the slope of the dew line may, however, become nearly infinite in the transition from b- to o-fluids it is more appropriate to consider the inverse slope of the dew line as quantitative measure. Hence, we define as measure for the skewness the inverse overhanging steepness (IOS) as

$$\mathrm{IOS} = (s''_{\max} - s''_{\min}) / [T(s''_{\max}) - T(s''_{\min})]. \quad (1)$$

Data for the critical temperature T_c, the critical pressure p_c, the acentric factor ω, the IOS and for the isobaric ideal gas heat capacity c_p^0 of all organic PFC working fluids considered in this paper are compiled in Table 1. The c_p^0-values were taken at $T/T_c = 0.7$ in analogy to the acentric factor ω. The values of ω and IOS are obtained from the molecular based equations of state (EOS) BACKONE (B1) [22,57,58] and PC-SAFT (PC) [59]. In passing, we note that the PC-SAFT predictions for the isobaric heat capacities of the saturated liquid siloxanes are in satisfying agreement with new experimental data [68]. For some fluids (n-butane, neopentane, R245ca, isopentane, n-pentane, toluene) we can compare the IOS values from Table 1 with IOS values obtained from reference equations of state (REOS) compiled in [69]. The average deviation in IOS is 0.0041 with a maximum deviation of 0.0086 for R245ca [70] and a minimum deviation of 0.0004 for toluene [71]; the references quote the original REOS papers.

Table 1 shows that within a given class of fluids (n-alkanes, aromates, linear siloxanes) the IOS increases with the number of atoms in the molecule as claimed in [41], whilst molecules with the same number of atoms from different classes may have rather different IOS, as e.g. cyclopentane and toluene. More interesting, however, is the finding that fluids from different classes with similar c_p^0 values have also similar IOS values, as e.g. n-butane and cylopentane, or n-pentane and toluene, or MM and butylbenzene. This finding can be a useful tool for a semi-quantitative estimate of the skewness of the VLE curve in the T,s-diagram.

3. Power flash cycles

3.1. Configuration of the PFC-system

The PFC-system is shown in Fig. 1 and consists of the power flash cycle to which heat is supplied from the heat carrier and removed by the cooling agent.

The PFC-plants considered here use a pure substance as working fluid and consist of a pump, a heater, a two-phase expander and a condenser or a cooler-condenser and eventually an internal heat exchanger (IHE). In state 1 the working fluid is a saturated liquid with temperature T_1 at the vapour pressure p_1. Then the liquid is pressurized by the pump to pressure p_2 and arrives at state 2 in the homogeneous liquid with a temperature T_2 being slightly above T_1. Thereafter, the liquid enters the heater where it is heated up isobarically just to its boiling point at pressure p_2 which is state 3. The temperature T_3 is the boiling temperature at pressure p_2. At state 3 the fluid enters the two-phase expander where it expands in a flash evaporation from p_2 down to p_1 at state 4. During this flash evaporation the working fluid delivers power. Depending on the working fluid, state 4 may be either in the wet or in the dry vapour region as will be shown in Subsection 3.2. If state 4 is in the wet vapour region, the temperature of the working fluid T_4 is equal to T_1 and its vapour content is denoted by x. Starting in this case from state 4 the wet vapour is completely condensed till it reaches state 1. If state 4 is in the dry vapour region, its temperature T_4 is higher than T_1. In case that T_4 is considerably higher than T_2 heat can be transferred in an IHE from the vapour between states 4 and 4a to the liquid between states 2 and 2a. Finally, the vapour is cooled down from state 4 or 4a at constant pressure p_1 to its dew point and thereafter completely condensed till it reaches state 1.

As already mentioned, the heat is supplied to the PFC-plant from a heat carrier which enters the heater at temperature T_5 and leaves

Table 1
Critical temperatures T_c, critical pressures p_c, acentric factors ω, inverse overhanging steepnesses IOS and isobaric ideal heat capacities c_p^0 of organic PFC working fluids. The c_p^0-values are taken at $T/T_c = 0.7$. The values of ω and IOS are obtained from the molecular based equations of state BACKONE (B1) and PC-SAFT (PC).

Substance	CAS no EC no	T_c (K)	p_c (MPa)	ω	IOS (J/molK^2)	c_p^0 (J/mol K)	EOS type, source	c_p^0 source
n-Butane	106-97-8 203-448-7	425.20	3.922	0.212	0.0500	100	B1 [57]	[60]
Neopentane (2,2-Dimethylpropane)	463-82-1 207-343-7	433.8	3.2	0.197	0.1089	124	B1 [57]	[61]
R245ca (1,1,2,2,3-Pentafluoropropane)	679-86-7 N/A	447.57	3.92	0.347	0.0821	121	B1 [58]	[62]
Isopentane (2-Methylbutane)	78-78-4 201-142-8	460.90	3.39	0.222	0.1081	127	B1 [57]	[61]
n-Pentane	109-66-0 203-692-4	469.65	3.370	0.248	0.1137	133	B1 [57]	[63]
Cyclopentane	287-92-3 206-016-6	511.7	4.51	0.193	0.0589	102	B1 [22]	[64]
MM	107-46-0 203-492-7	518.70	1.925	0.420	0.331	264	PC [59]	[65]
MDM	107-51-7 203-497-4	564.13	1.415	0.536	0.591	394	PC [59]	[65]
Toluene	108-88-3 203-625-9	591.80	4.109	0.263	0.1122	144	B1 [22]	[66]
MD2M	141-62-8 205-491-7	599.40	1.190	0.658	0.812	503	PC [59]	[65]
m-Xylene	108-38-3 203-576-3	617.05	3.541	0.321	0.165	179	B1 [22]	[66]
Ethylbenzene	100-41-4 202-849-4	617.20	3.609	0.301	0.169	186	B1 [22]	[67]
MD3M	141-63-9 205-492-2	629.00	0.945	0.720	1.131	668	PC [59]	[65]
Butylbenzene	104-51-8 203-209-7	660.05	2.887	0.392	0.276	258	B1 [22]	[61]

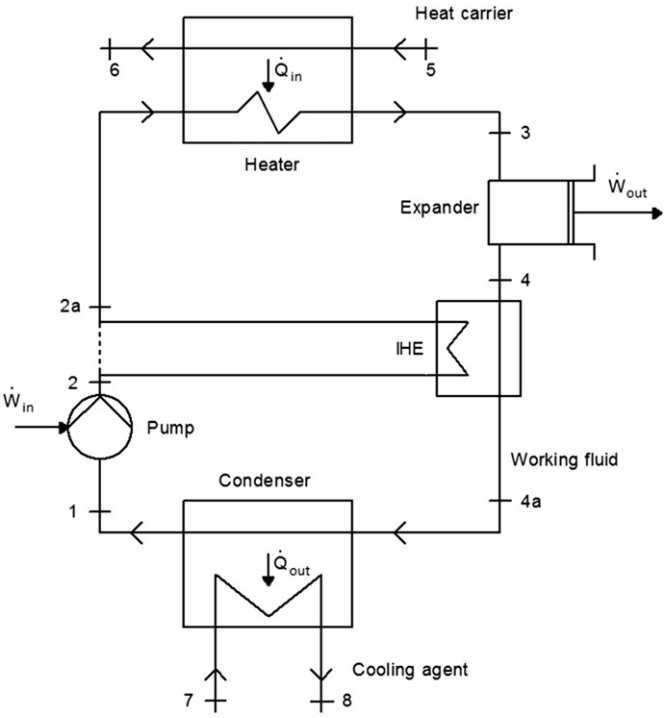

Fig. 1. Configuration of the PFC – system.

it at temperature T_6. The heat is removed by a cooling agent which enters the condenser at temperature T_7 and leaves it at temperature T_8.

The two-phase expander is the technically most challenging component and may be a turbine, a scroll expander, a screw expander or a reciprocating engine. A review of expanders was given in 1993 by Smith [41] who somewhat later described the design of high-efficiency two-phase screw expanders [46]. Recent developments for a screw-type engine are described in [47] and for a reciprocating engine in [48,50,52]. We believe that the latter is presently the most promising two-phase expander.

3.2. Different types of power flash cycles

In order to understand a PFC it is helpful to consider cycles with different working fluids in the *T,s*-diagram. In Figs. 2–4 results are

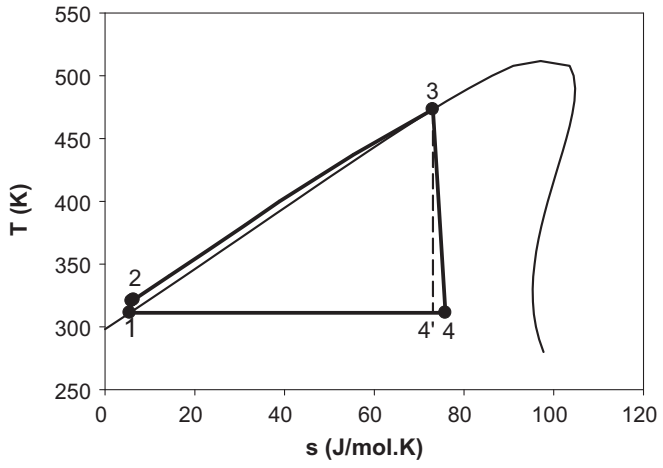

Fig. 2. *T,s*-diagram of optimized PFC with cyclopentane ($T_5 = 493.15$ K, $T_1 = 311.15$ K, IOS = 0.059, $T_c = 511.7$).

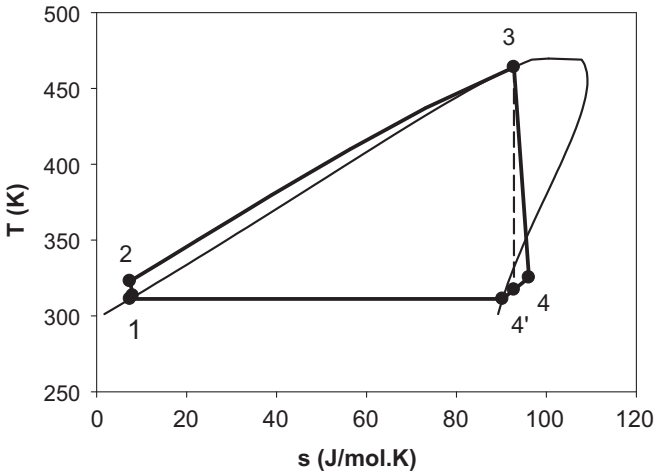

Fig. 3. *T,s*-diagram of optimized PFC with n-pentane ($T_5 = 493.15$ K, $T_1 = 311.15$ K, IOS = 0.107, $T_c = 469.65$ K).

shown for three optimized PFC-systems for case IV with heat carrier inlet temperature $T_5 = 493.15$ K and minimum cycle temperature $T_1 = 311.15$ K. The working fluids have increasing IOS and are cyclopentane, n-pentane, and MM. The optimization criterion will be explained later.

In Fig. 2 the PFC for cyclopentane (IOS = 0.059 J/molK^2, $T_c = 511.7$) is shown. The end point 4 of the flash expansion is in the wet vapour region with a vapour content $x = 0.76$. The shape of the PFC in the *T,s*-diagram is rather similar to that of water with the difference that water has for the same case IV at point 4 only a vapour content of $x = 0.25$ [53]. Because of its shape in the *T,s*-diagram this type of PFC is called TLC as points 1 and 2 are close together in the *T,s*-diagram.

The PFC for n-pentane (IOS = 0.107 J/molK^2, $T_c = 469.65$ K) is shown in Fig. 3. The power flash passes through the wet vapour region and ends at point 4 in the dry vapour region with $T_4 = 325$ K. Because of its shape in the *T,s*-diagram this type of PFC is called QLC. As T_4 is only 12 K higher than T_2 it is not rewarding to use an IHE.

In Fig. 4 the PFC for MM (IOS = 0.331 J/molK^2, $T_c = 518.7$ K) is shown. The power flash expansion passes through the wet vapour region and ends at point 4 in the dry vapour region which has the temperature $T_4 = 353$ K. Because of its shape in the *T,s*-diagram this

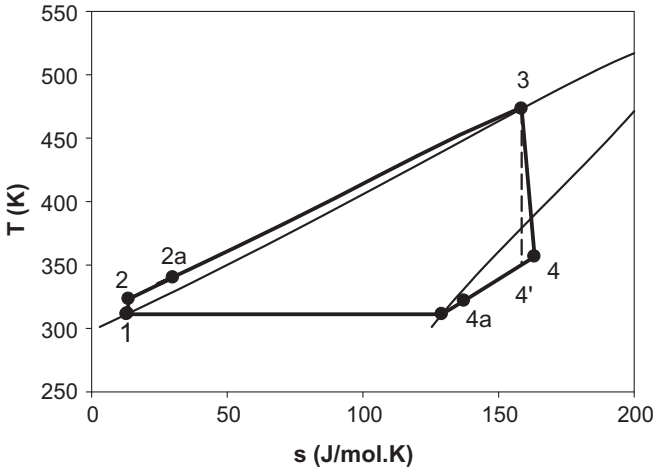

Fig. 4. *T,s*-diagram of optimized PFC with MM ($T_5 = 493.15$ K, $T_1 = 311.15$ K, IOS = 0.331, $T_c = 518.7$ K). In an IHE heat can be transferred from the vapour between states 4 and 4a to the liquid between states 2 and 2a.

type of PFC is called QLC. As T_4 is considerably larger than T_2 it may be rewarding to transfer heat in an IHE from the vapour between states 4 and 4a to the liquid between states 2 and 2a.

Summarizing, if the end point of the expansion, state 4, is in the wet vapour region the PFC is called TLC. If state 4 is in the dry vapour region the PFC is called QLC which depending on the temperature T_4 may be designed without (QLC-) or with IHE (QLC+).

4. Thermodynamics of PFC-systems

The thermodynamic calculations for PFC-systems are similar to that of ORC- [8,22] and TLC-systems [53]. In the following, the quantities T_i, p_i, h_i, s_i and v_i denote the temperature, the pressure, the specific enthalpy, the specific entropy and the specific volume at state point i and the quantities w_{ij} and q_{ij} denote the specific work and heat in the process from state point i to state point j. The hypothetical state point 2′ lies on the isobar p_2 and has the same entropy as state 1, $s'_2 = s_1$, the hypothetical state point 4′ lies on the isobar p_1 and has the same entropy as state 3, $s'_4 = s_3$. Moreover, we assume throughout the paper for the isentropic pump efficiency $\eta_{sP} = (h'_2 - h_1)/(h_2 - h_1) = 0.65$, for the isentropic expander efficiency $\eta_{s,E} = (h_4 - h_3)/(h'_4 - h_3) = 0.85$ and for all pinch point temperature differences $\Delta T = 10$ K.

4.1. Process quantities of the PFC

The specific work transferred to the cycle in the pump is $w_{12} = h_2 - h_1$ and specific work delivered from the expander is $w_{34} = h_4 - h_3$. Hence, the net specific work is $w = w_{12} + w_{34}$. For a mass flow rate of the working fluid $\dot{m}_{WF}$ the net power output is

$$|\dot{W}| = \dot{m}_{WF}|w_{12} + w_{34}| \tag{2}$$

and the volume flow rate $\dot{V}_i$ at a given state i with specific volume v_i is given by

$$\dot{V}_i = \dot{m}_{WF} v_i. \tag{3}$$

For easy comparison we refer all flow rates throughout the paper to a net power output $|\dot{W}|$ of 1 MW.

Whilst the transferred works and the net power output are independent from the use of an IHE, the situation is different for the transferred heats. In case without IHE the heat flow rate to the cycle is $\dot{Q}_{23} = \dot{m}_{WF}\, q_{23}$ with $q_{23} = h_3 - h_2$. The heat flow rate from the cycle is $\dot{Q}_{41} = \dot{m}_{WF}\, q_{41}$ with $q_{41} = h_1 - h_4$ and the thermal efficiency of the cycle η_{th} is

$$\eta_{\text{th}} = |w_{12} + w_{34}|/q_{23} \quad \text{(without IHE)}. \tag{4}$$

In case with IHE states 2 and 4 have to be replaced by states 2a and 4a. Then the heat flow rate to the cycle is $\dot{Q}_{2a3} = \dot{m}_{WF}\, q_{2a3}$ with $q_{2a3} = h_3 - h_{2a}$. The heat flow rate from the cycle is $\dot{Q}_{4a1} = \dot{m}_{WF}\, q_{4a1}$ with $q_{4a1} = h_1 - h_{4a}$ and the thermal efficiency of the cycle η_{th} is

$$\eta_{\text{th}} = |w_{12} + w_{34}|/q_{2a3} \quad \text{(with IHE)}. \tag{5}$$

4.2. Heat transfers to and from the PFC

Heat transfer processes to and from the working fluid have been discussed for ORC and TLC in Section 4 of [53] in detail. Here we follow this previous work and assume throughout the paper that all heat transfer processes to and from the working fluid of the PFC are adiabatic. Hence, we have $\dot{Q}_{56} = -\dot{Q}_{23}$ and $\dot{Q}_{78} = -\dot{Q}_{41}$ without IHE and $\dot{Q}_{56} = -\dot{Q}_{2a3}$ and $\dot{Q}_{78} = -\dot{Q}_{4a1}$ with IHE. Note that $\dot{Q}_{56}$ has negative sign whilst $\dot{Q}_{78}$ has positive sign. Moreover, we assume that the heat carrier (HC) and the cooling agent (CA) have constant heat capacities c_p. In order to express the heat flow rates $\dot{Q}_{56}$ and $\dot{Q}_{78}$ it is convenient to use heat capacity flow rates $\dot{C} = \dot{m}c_p$. Therewith the absolute value of the heat flow rate $|\dot{Q}_{56}|$ from the heat carrier to the working fluid is

$$|\dot{Q}_{56}| = \dot{C}_{HC}(T_5 - T_6), \tag{6}$$

and the heat flow rate $\dot{Q}_{78}$ from the working fluid to the cooling agent is

$$\dot{Q}_{78} = \dot{C}_{CA}(T_8 - T_7) \tag{7}$$

For the heat transfer to a TLC a T, $\Delta\dot{H}$-diagram for two cases is shown in Fig. 4 of [53]. These diagrams look similar for all PFC, only in case of an IHE the cold end of the working fluid is shifted from T_2 to T_{2a}.

For the heat transfer from the working fluid, we have to distinguish between TLC and QLC processes. For the TLC, a T, $\Delta\dot{H}$-diagram is shown in Fig. 7 of [53]. For the QLC with IHE the T, $\Delta\dot{H}$-diagram is the same as for an ORC with IHE which is shown in Fig. 8 of [53], in case of no IHE state 4a has to be replaced in Fig. 8 of [53] by state 4. In both cases of QLC one has to make separate balances for the cooling and the condensation as described in [53].

4.3. Energy and exergy equations

4.3.1. Energy equations

From the first law of thermodynamics and the assumption of adiabatic heat transfer in the PFC-systems one obtains

$$|\dot{Q}_{56}| - \dot{Q}_{78} = |\dot{W}|, \tag{8}$$

which yields for the case of $|\dot{W}| = 1$ MW used throughout this paper $\dot{Q}_{78} = |\dot{Q}_{56}| - 1$ MW. Next, one gets from the definitions of the thermal efficiency η_{th} the relation

$$|\dot{W}| = |\dot{Q}_{56}|\eta_{\text{th}}, \tag{9}$$

which says that the net power output is the product of the heat flow rate $|\dot{Q}_{56}|$ transferred from the heat carrier to the working fluid times the thermal efficiency η_{th} of the PFC.

4.3.2. Exergy equations

As exergy equations have been given in detail in [53] we repeat here only the most important ones. Generally, for a state point i and a mass flow rate $\dot{m}$ the exergy flow rate $\dot{E}_i$ is given as

$$\dot{E}_i = \dot{m}e_i, \tag{10}$$

where e_i is the specific exergy at state i which is known to be

$$e_i = (h_i - h_u) - T_u(s_i - s_u), \tag{11}$$

where the subscript u refers to the conditions of the environment. Finally, using the heat capacity flow rate $\dot{C} = \dot{m}c_p$ one obtains for the exergy flow rate

$$\dot{E}_i = \dot{C}[(T_i - T_u) - T_u \ln(T_i/T_u)]. \tag{12}$$

The latter equation can now be specified for the exergy flow rates $\dot{E}_5$, $\dot{E}_6$, $\dot{E}_7$, and $\dot{E}_8$ at the inlet and outlet of the heat carrier and the cooling agent by using the appropriate temperature T_i and the appropriate heat capacity flow rate $\dot{C}_{HC}$ or $\dot{C}_{CA}$.

With Eq. (12) exergy efficiencies can now be formulated. The exergy efficiency for power production ξ_p is defined as ratio of the

net power output $|\dot{W}|$ to the incoming exergy flow rate of the heat carrier $\dot{E}_5$ and is obtained as

$$\xi_P = |\dot{W}|/\{\dot{C}_{HC}[(T_5 - T_u) - T_u \ln(T_5/T_u)]\}, \quad (13)$$

whilst the total exergy efficiency ξ defined as ratio of all outgoing exergy flows to all incoming exergy flows is given as

$$\xi = (|\dot{W}| + \dot{E}_6 + \dot{E}_8)/(\dot{E}_5 + \dot{E}_7). \quad (14)$$

5. Results and discussion

We consider five cases specified by the inlet temperature of the heat carrier T_5 and the inlet temperature of the cooling agent T_7. The inlet temperature pairs (T_5, T_7) are for case I (350 °C, 62 °C), for case II (280 °C, 62 °C), for case III (280 °C, 15 °C), for case IV (220 °C, 15 °C) and for case V (150 °C, 15 °C). Organic PFC are compared with water TLC [53], with optimized ORC [53] and also with water CRC. For the thermodynamic data of the organic working fluids we use BACKONE [72] and PC-SAFT [59] with details given in Table 1, for water we take the Wagner EOS [73] via the NIST webbook [69].

In all calculations we assume for $T_1 = T_7 + 23$ K, for the environmental temperature $T_u = 15$ °C, for the isentropic pump efficiency $\eta_{s,P} = 0.65$, for the isentropic expander efficiency $\eta_{s,E} = 0.85$, for all pinch point temperature differences $\Delta T = 10$ K and also that all heat exchangers are adiabatic.

Optimized results of the present calculations for organic PFC and for water CRC are displayed together with previous optimized results [53] for water TLC and optimized ORC in Tables 2–6. The optimization criterion for these systems is that the exergy efficiency for power production ξ_p becomes a maximum. For completeness, we include for all QLC+ also the results of the corresponding QLC− in brackets.

The quantities given are the critical temperature T_c of the working fluid and its IOS, the cycle type, the cycle temperatures and pressures T_2, T_{2a}, T_3, T_4, p_1, p_3, the expander inlet and outlet volume flow rates $\dot{V}_3$, $\dot{V}_4$, the mass flow rate $\dot{m}_{WF}$, the heat transferred in the IHE $\dot{Q}_{2,2a}$, the vapour content at the expander outlet x, the thermal efficiency of the cycle η_{th}, the heat carrier outlet temperature T_6, the temperature of the heat carrier at the pinch point T_p, the absolute value of the heat transferred to the working fluid $|\dot{Q}_{56}|$, the heat capacity flow rate of the heat carrier $\dot{C}_{HC}$, the cooling agent outlet temperature T_8, the heat capacity flow rate of the cooling agent $\dot{C}_{CA}$, the total exergy efficiency ξ, and the exergy efficiency for power production ξ_P. As already said all flow rates are given for a net power output $|\dot{W}|$ of 1 MW.

Quantities that can be easily calculated from the data in the tables are $\dot{Q}_{78} = |\dot{Q}_{56}| - 1$ MW, $T_{4a} = T_2 + 10$ K. Moreover $\dot{E}_5$, $\dot{E}_6$, $\dot{E}_7$, $\dot{E}_8$ can be calculated from Eq. (12) as $\dot{C}_{HC}$ and $\dot{C}_{CA}$ and all temperatures T_5 to T_8 and T_u are also given.

Comparison of the bracketed QLC− with the corresponding QLC+ results in Tables 2–5 shows that the total exergy efficiency ξ is always smaller for QLC− as it has to be. The exergy efficiency for power production ξ_p is also smaller for QLC− for a lower pinch point temperature T_p but identical with the QLC+ value in case of the same T_p. The latter case may be considered at a first glance as an advantage for QLC− because according to Fig. 1 one needs only two heat exchangers for QLC− instead of three for QLC+. But the total amount of heat to be transferred for QLC− is $|\dot{Q}_{tot,\ QLC-}| = |\dot{Q}_{23}| + |\dot{Q}_{41}| = |\dot{Q}_{2a3}| + |\dot{Q}_{4a1}| + 2|\dot{Q}_{22a}|$, whilst for QLC+ it is only $|\dot{Q}_{tot,\ QLC+}| = |\dot{Q}_{2a3}| + |\dot{Q}_{4a1}| + |\dot{Q}_{22a}|$. Hence, there is no advantage of QLC− over QLC+ in case that T_4 is sufficiently higher than T_2 as in Fig. 4 and we will not include the bracketed QLC− results in the subsequent discussions of the case studies.

5.1. Case I: $T_5 = 350$ °C, $T_7 = 62$ °C

Let us first consider the PFC-systems. From Table 2 we learn that the water TLC has the highest exergy efficiency for power

Table 2
Optimized results for case I ($T_5 = 623.15$ K, $T_7 = 335.15$ K, $T_1 = 358.15$ K, $T_u = 288.15$ K). All flow rates are given for a net power output $|\dot{W}|$ of 1 MW.

	Butylbenzene	Water[a]	MD3M	Ethylbenzene	m-Xylene	MD2M	Toluene	MDM	MM	Water	Cyclopentane[a]
T_c (K)	660	647	629	617	617	599	592	564	519	647	512
IOS	0.276	–	1.131	0.169	0.165	0.812	0.112	0.591	0.331	–	0.059
Cycle type	QLC+ (QLC−)	TLC	QLC+ (QLC−)	QLC+ (QLC−)	QLC+ (QLC−)	QLC+ (QLC−)	QLC+ (QLC−)	QLC+ (QLC−)	QLC+ (QLC−)	CRC	ORCs2+
T_2 (K)	358.83	360.21	358.28	359.66	359.61	358.46	360.46	358.80	359.62	358.41	362.28
T_{2a} (K)	401.15	–	434.01	390.43	386.08	429.72	380.76	428.20	411.07	–	384.29
T_3 (K)	588	590	534	588	588	537	583	534	515	613	529
T_4 (K)	419.44	358.15	453.68	409.26	403.95	450.55	397.28	449.57	431.70	358.15	401.00
p_1 (kPa)	3.94	57.87	0.57	20.26	18.44	2.37	46.04	11.26	62.92	57.87	289
p_3 (kPa)	1134	10,821	195	2485	2402	431	3622	912	1887	1400	5412
$\dot{V}_3$ (l/s)	16.27	7.00	37.69	18.14	18.15	38.74	21.33	41.93	55.68	366.02	51.0
$\dot{V}_4$ (l/s)	60,151	4994	396,435	14,231	15,469	109,174	7051	28,274	7053	5114	1778
$\dot{m}_{WF}$ (kg/s)	9.14	4.72	23.01	9.06	9.08	21.55	9.18	20.28	20.56	1.86	11.35
$\dot{Q}_{2,2a}$ (MW)	0.77	–	3.27	0.56	0.48	2.82	0.36	2.79	2.23	–	0.54
x	Dry	0.37	Dry	Dry	Dry	Dry	Dry	Dry	Dry	0.97	Dry
η_{th}	0.230 (0.195)	0.198	0.206 (0.123)	0.223 (0.198)	0.220 (0.199)	0.207 (0.130)	0.216 (0.200)	0.203 (0.129)	0.181 (0.129)	0.194	0.186
T_6 (K)	411.67 (373.97)	370.53	444.01 (368.28)	402.12 (374.49)	397.78 (373.91)	439.72 (368.46)	393.89 (376.00)	438.20 (368.80)	421.07 (369.62)	447.76	394.29
T_p (K)	433 (433)	414	444 (368)	446 (446)	442 (442)	440 (368)	452 (452)	438 (369)	421 (370)	477	394
$|\dot{Q}_{56}|$ (MW)	4.34 (5.12)	5.05	4.85 (8.12)	4.48 (5.04)	4.54 (5.02)	4.84 (7.67)	4.64 (5.00)	4.93 (7.72)	5.54 (7.75)	5.15	5.37
$\dot{C}_{HC}$ (MW/K)	0.0205 (0.0205)	0.0200	0.0271 (0.0319)	0.0203 (0.0203)	0.0201 (0.0201)	0.0264 (0.0301)	0.0202 (0.0202)	0.0267 (0.0304)	0.0274 (0.0306)	0.0294	0.0234
T_8 (K)	348.77 (351.92)	348.15	349.49 (361.68)	348.75 (350.94)	348.73 (350.58)	349.37 (359.81)	348.74 (350.09)	349.39 (359.48)	349.36 (356.26)	348.15	348.94
$\dot{C}_{CA}$ (MW/K)	0.245	0.312	0.268	0.256	0.260	0.270	0.268	0.276	0.319	0.320	0.317
ξ	0.885 (0.863)	0.873	0.850 (0.765)	0.882 (0.868)	0.881 (0.869)	0.851 (0.775)	0.878 (0.869)	0.847 (0.774)	0.827 (0.774)	0.840	0.844
ξ_p	0.432 (0.432)	0.443	0.328 (0.278)	0.438 (0.438)	0.441 (0.441)	0.336 (0.295)	0.438 (0.438)	0.332 (0.292)	0.324 (0.290)	0.302	0.378

[a] Results are from [53].

Table 3
Optimized results for case II ($T_5 = 553.15$ K, $T_7 = 335.15$ K, $T_1 = 358.15$ K, $T_u = 288.15$ K). All flow rates are given for a net power output $|\dot{W}|$ of 1 MW.

	Butylbenzene	Water[a]	Ethylbenzene	m-Xylene	MD2M	Toluene	MDM	MM	Cyclopentane	Water	Cyclopentane[a]
T_c (K)	660	647	617	617	599	592	564	519	512	647	512
IOS	0.276	–	0.169	0.165	0.812	0.112	0.591	0.331	0.059	–	0.059
Cycle type	TLC	TLC	TLC	TLC	QLC+ (QLC-)	TLC	QLC+ (QLC-)	QLC+ (QLC-)	TLC	CRC	ORCo2+
T_2 (K)	358.45	359.08	358.89	358.86	358.35	359.36	358.60	359.46	361.48	358.27	360.63
T_{2a} (K)	–	–	–	–	406.70	–	405.31	401.97	–	–	380.27
T_3 (K)	535	534	535	535	514	533	512	508	510	543	489.00
T_4 (K)	358.15	358.15	358.15	358.15	424.30	358.15	423.17	420.83	358.15	358.15	396.41
p_1 (kPa)	3.94	57.87	20.26	18.44	2.37	46.04	11.26	62.92	288.80	57.87	288.8
p_3 (kPa)	507	4757	1221	1172	278	1914	627	1691	4418	700	3342
$\dot{V}_3$ (l/s)	23.08	10.40	24.77	24.93	43.01	26.92	45.06	54.56	45.41	874.18	121.0
$\dot{V}_4$ (l/s)	80,450	6540	18,937	20,539	122,980	9349	31,753	7388	2130	6873	1937
$\dot{m}_{WF}$ (kg/s)	14.61	8.13	15.05	15.14	25.79	15.69	24.24	22.14	15.88	2.49	12.53
$\dot{Q}_{2,2a}$ (MW)	–	–	–	–	2.26	–	2.21	1.97	–	–	0.53
x	0.98	0.28	0.92	0.90	Dry	0.87	Dry	Dry	0.98	0.98	Dry
η_{th}	0.166	0.159	0.164	0.164	0.179 (0.127)	0.163	0.176 (0.127)	0.170 (0.128)	0.150	0.152	0.173
T_6 (K)	375.64	369.15	374.58	374.08	416.70 (368.35)	374.48	415.31 (368.60)	411.97 (369.47)	373.67	431.81	408.70
T_p (K)	448	387	451	449	417 (368)	447	415 (369)	412 (369)	413	447	483
$\lvert\dot{Q}_{56}\rvert$ (MW)	6.01	6.31	6.08	6.09	5.59 (7.85)	6.15	5.69 (7.90)	5.88 (7.83)	6.66	6.58	5.79
$\dot{C}_{HC}$ (MW/K)	0.0338	0.0343	0.0341	0.0340	0.0410 (0.0425)	0.0344	0.0413 (0.0428)	0.0416 (0.0426)	0.0371	0.0543	0.0401
T_8 (K)	348.15	348.15	348.15	348.15	349.35 (356.32)	348.15	349.36 (356.05)	349.35 (355.00)	348.15	348.15	348.85
$\dot{C}_{CA}$ (MW/K)	0.385	0.408	0.391	0.391	0.323	0.396	0.330	0.344	0.436	0.429	0.350
ξ	0.886	0.881	0.884	0.884	0.878 (0.833)	0.882	0.875 (0.832)	0.870 (0.833)	0.867	0.852	0.890
ξ_p	0.383	0.378	0.381	0.382	0.316 (0.305)	0.377	0.314 (0.303)	0.312 (0.304)	0.350	0.239	0.332

[a] Results are from [53].

Table 4
Optimized results for case III ($T_5 = 553.15$ K, $T_7 = 288.15$ K, $T_1 = 311.15$ K, $T_u = 288.15$ K). All flow rates are given for a net power output $|\dot{W}|$ of 1 MW.

	Water[a,b]	Ethylbenzene	m-Xylene	Toluene	MDM	MM	Cyclopentane	Water	Cyclopentane[a]
T_c (K)	647	617	617	592	564	519	512	647	512
IOS	–	0.169	0.165	0.112	0.591	0.331	0.059	–	0.059
Cycle type	TLC	TLC	TLC	TLC	QLC+ (QLC−)	QLC+ (QLC−)	QLC−	CRC	ORCo2+
T_2 (K)	311.90	311.79	311.78	312.22	311.45	312.14	314.31	311.20	312.96
T_{2a} (K)	–	–	–	–	368.34	366.48	–	–	337.65
T_3 (K)	534	528	529	527	496	498	510	543	470.00
T_4 (K)	311.15	311.15	311.15	311.15	388.69	388.40	315.94	311.15	357.09
p_1 (kPa)	6.63	2.58	2.28	7.16	1.20	10.43	68.88	6.63	68.88
p_3 (kPa)	4757	1100	1071	1759	468	1441	4418	350	2546
$\dot{V}_3$ (l/s)	6.24	15.94	15.92	17.06	28.56	31.76	26.65	1231	113.7
$\dot{V}_4$ (l/s)	33,546	87,736	97,612	35,293	185,330	26,805	4944	35,374	4824
$\dot{m}_{WF}$ (kg/s)	4.88	9.85	9.81	10.13	16.28	14.13	9.32	1.74	7.98
$\dot{Q}_{2,2a}$ (MW)	–	–	–	–	1.71	1.51	–	–	0.38
x	0.32	0.95	0.93	0.89	Dry	Dry	Dry	0.94	Dry
η_{th}	0.211	0.215	0.216	0.214	0.228 (0.164)	0.228 (0.170)	0.209	0.202	0.2329
T_6 (K)	322.39	329.53	329.91	329.62	378.34 (321.45)	376.48 (322.14)	333.66	398.30	372.89
T_p (K)	388	411	413	412	378 (321)	376 (322)	413	421	480
$\lvert\dot{Q}_{56}\rvert$ (MW)	4.75	4.65	4.64	4.67	4.38 (6.09)	4.38 (5.88)	4.78	4.95	4.29
$\dot{C}_{HC}$ (MW/K)	0.0206	0.0208	0.0208	0.0209	0.0251 (0.0263)	0.0248 (0.0254)	0.0218	0.0320	0.0238
T_8 (K)	301.15	301.15	301.15	301.15	302.16 (309.21)	302.11 (308.29)	301.35	301.15	301.65
$\dot{C}_{CA}$ (MW/K)	0.288	0.281	0.280	0.283	0.242	0.242	0.286	0.304	0.245
ξ	0.706	0.709	0.710	0.706	0.710 (0.604)	0.711 (0.617)	0.688	0.660	0.721
ξ_p	0.631	0.624	0.625	0.620	0.517 (0.494)	0.524 (0.510)	0.596	0.406	0.545

[a] Results are from [53].
[b] Contains corrections for some values of [53].

production $\xi_P = 0.443$ and the smallest volume flow rate $\dot{V}_4 = 4994$ l/s at the outlet of the expander. The aromates toluene, m-xylene, ethylbenzene, butylbenzene exhibit QLC and show nearly the same ξ_P as water in TLC with an average value 0.437 ± 0.003. The volume flow rate $\dot{V}_4 = 7051$ l/s for toluene is acceptable, but it increases for the other aromates with T_c up to $\dot{V}_4 = 60{,}151$ l/s for butylbenzene. The siloxanes MM, MDM, MD2M, MD3M exhibit also QLC as expected because of their large IOS values. They show lower ξ_P values with an average value 0.330 ± 0.004. The volume flow rate $\dot{V}_4 = 7053$ l/s is acceptable for MM but increases for others dramatically with T_c up to $\dot{V}_4 = 396{,}435$ l/s for MD3M. Hence for this case water is the best working fluid for PFC.

Let us now compare the PFC with the water CRC and the cyclopentane ORC. In [53] it was already pointed out that ξ_P for the water TLC is larger by 17% than for the cyclopentane ORC. On the other hand we see that the volume flow $\dot{V}_4$ of the ORC amounts only 36% of the water TLC value. Considering the water CRC we see that its ξ_P is only 70% of that for the water TLC and 80% of that for the cyclopentane ORC.

Finally, it is interesting that the values for the total exergy efficiency ξ are rather high with an average value of 0.86 ± 0.02.

5.2. Case II: $T_5 = 280$ °C, $T_7 = 62$ °C

From Table 3 we see that the PFC of the aromates are now of TLC type with an average value of ξ_P for all aromates of 0.381 ± 0.002 and the highest value 0.383 for butylbenzene. For the water TLC ξ_P has the slightly lower value 0.378. Looking now on the volume flow

Table 5
Optimized results for case IV ($T_5 = 493.15$ K, $T_7 = 288.15$ K, $T_1 = 311.15$ K, $T_u = 288.15$ K). All flow rates are given for a net power output $|\dot{W}|$ of 1 MW.

	Water[a]	Ethylbenzene	Toluene	MDM	MM	Cyclopentane	n-Pentane	Isopentane	R245ca	Water	n-Butane[a]
T_c (K)	647	617	592	564	519	512	470	461	448	647	425
IOS	–	0.169	0.112	0.591	0.331	0.059	0.114	0.108	0.082	–	0.050
Cycle type	TLC	TLC	TLC	QLC+ (QLC-)	QLC+ (QLC-)	TLC	QLC-	QLC-	TLC	CRC	ORCs2+
T_2 (K)	311.43	311.41	311.62	311.34	311.76	312.93	313.29	313.52	313.42	311.17	314.86
T_{2a} (K)	–	–	–	345.08	336.82	–	–	–	–	–	321.54
T_3 (K)	479	475	475	472	470	469	464	458	445	483	443.60
T_4 (K)	311.15	311.15	311.15	361.56	352.67	311.15	325.27	326.43	311.15	311.15	333.55
p_1 (kPa)	6.63	2.58	7.16	1.20	10.43	68.89	109.25	142.99	163.9	6.63	359.7
p_3 (kPa)	1754	449	776	292	894	2508	3045	3197	3679	150	4706
$\dot{V}_3$ (l/s)	9.53	24.64	25.81	32.43	34.79	31.95	39.88	45.48	43.88	3393	74.8
$\dot{V}_4$ (l/s)	43,550	114,143	45,852	209,935	31,205	6429	4318	3584	3216	47,331	1711
$\dot{m}_{WF}$ (kg/s)	8.18	16.92	17.36	19.83	18.15	16.22	13.07	14.26	29.56	2.30	13.90
$\dot{Q}_{2,2a}$ (MW)	–	–	–	1.21	0.87	–	–	–	–	–	0.24
x	0.25	0.72	0.68	Dry	Dry	0.76	Dry	Dry	0.97	0.95	Dry
η_{th}	0.171	0.174	0.173	0.195 (0.158)	0.188 (0.161)	0.169	0.166	0.162	0.150	0.159	0.161
T_6 (K)	321.42	326.67	326.58	355.11 (322.41)	347.08 (323.12)	328.43	327.24	325.56	323.42	381.68	333.18
T_p (K)	321	392	393	361 (362)	365 (365)	390	386	367	323	394	368.16
$\lvert\dot{Q}_{56}\rvert$ (MW)	5.86	5.75	5.77	5.12 (6.33)	5.33 (6.20)	5.92	6.01	6.18	6.66	6.28	6.22
$\dot{C}_{HC}$ (MW/K)	0.0341	0.0345	0.0347	0.0371 (0.0371)	0.0365 (0.0365)	0.0359	0.0362	0.0369	0.0393	0.0564	0.0389
T_8 (K)	301.15	301.15	301.15	302.15 (306.27)	302.08 (304.85)	301.15	302.09	302.22	301.15	301.15	302.13
$\dot{C}_{CA}$ (MW/K)	0.374	0.365	0.367	0.294	0.311	0.378	0.359	0.368	0.436	0.406	0.373
ξ	0.681	0.685	0.682	0.724 (0.662)	0.708 (0.665)	0.666	0.664	0.652	0.611	0.644	0.627
ξ_p	0.584	0.578	0.575	0.537 (0.537)	0.547 (0.547)	0.555	0.551	0.541	0.508	0.354	0.513

[a] Results are from [53].

rates at the outlet of the expander we find for water $\dot{V}_4 = 6540$ l/s whilst for the aromates the lowest value is that for toluene being $\dot{V}_4 = 9349$ l/s but increases for the other aromates with T_c up to $\dot{V}_4 = 80{,}450$ l/s for butylbenzene. Toluene, however, has in comparison with water a marginally smaller $\xi_P = 0.377$. The siloxanes exhibit still QLC and show again low ξ_P with an average value $\xi_P = 0.312 \pm 0.004$. For MM the volume flow rate $\dot{V}_4 = 7392$ l/s is reasonable but increases dramatically with T_c up to $\dot{V}_4 = 122{,}980$ l/s already for MD2M so that there is no advantage for using siloxanes. In addition, we show PFC results for cyclopentane which are interesting. The cycle is of TLC type with $\xi_p = 0.350$ which is 93% of the water TLC value and has a rather low $\dot{V}_4 = 2130$ l/s. Note, however, that the maximum cycle temperature $T_3 = 510$ K is rather close to its critical temperature $T_c = 512$ K which may cause problems in a real process.

Let us now compare the PFC with the water CRC and the cyclopentane ORC. In [53] it was already pointed out that ξ_P for the water TLC is larger by 14% than for the cyclopentane ORC. On the other hand we see that the volume flow $\dot{V}_4$ at the outlet of the expander of the ORC amounts only 30% of the water TLC value. Considering the water CRC we see that its ξ_P is only 63% of that for the water TLC and 72% of that for the cyclopentane ORC, which confirms the claim that water CRC become worse with decreasing heat carrier inlet temperatures.

5.3. Case III: $T_5 = 280$ °C, $T_7 = 15$ °C

Table 4 shows that water in TLC has now again the highest $\xi_P = 0.631$. (Let us note that in [53] a calculation error occurred for case III in the water TLC which is corrected here.) The aromates exhibit TLC and have nearly the same ξ_P as water with an average value of 0.623 ± 0.002. A dramatic increase in ξ_P in comparison with case II is observed which amounts 67% for the water TLC and 61% for the aromates which is caused by lowering the temperature T_7 from 62 °C to 15 °C. As a consequence of this increase in ξ_P the mass flow rates $\dot{m}_{WF}$ for 1 MW net output decrease in comparison with case II and so do the volume flow rates $\dot{V}_3$. On the other hand, because of the low vapour pressures at T_1, the volume flow rates $\dot{V}_4$ become significantly larger. For water $\dot{V}_4$ becomes 33,546 l/s, for toluene $\dot{V}_4 = 35{,}293$ l/s, and for the other aromates the $\dot{V}_4$ values are still higher; consequently we did not include butylbenzene in Table 4. Looking on the siloxanes no advantages can be found. Their volume flow rates $\dot{V}_4$ are also rather high whilst their exergy efficiencies ξ_P are 17.5% lower than that of water. Cyclopentane exhibits now a QLC which has a similar T,s-diagram as shown in Fig. 3. The cycle yields a ξ_P value of 0.596 which is 94% of the ξ_P for the water TLC. Moreover, because the whole cycle runs at high reduced temperatures T/T_c the volume flow rate $\dot{V}_4$ is only 4944 l/s which is just 15% of that for water. The problem is again that in the optimized system the maximum cycle temperature $T_3 = 510$ K is rather close to its critical temperature $T_c = 512$ K.

We compare now the PFC-systems with the water CRC system and the cyclopentane ORC system. The water CRC shows again a small ξ_P and a slightly larger $\dot{V}_4$ than the water TLC. Considering the cyclopentane ORC it is seen that its ξ_P amounts to 86% to that of the water TLC and 91% to that of the cyclopentane QLC. The volume flow rates $\dot{V}_4$ of the QLC and of the ORC with cyclopentane are nearly the same. These results for cyclopentane indicate a certain convergence of PFC- and ORC-systems.

Finally, the average value for the total exergy efficiency ξ of all systems in Table 4 is 0.70 ± 0.02 which is remarkably smaller than in cases I and II.

5.4. Case IV: $T_5 = 220$ °C, $T_7 = 15$ °C

From Table 5 it is seen that the water TLC has again the highest ξ_P being 0.584 and that the aromates follow closely. On the other hand the volume flow rates $\dot{V}_4$ become now already 43,550 l/s for water and 45,852 l/s for toluene. The $\dot{V}_4$ values increase again for the higher aromates up to 713,235 l/s for butylbenzene and hence this fluid and m-xylene are not included in Table 5. For the siloxanes Table 5 presents results for MM and MDM which still exhibit QLC. Using an IHE we find for MM $\xi_P = 0.547$ which is 94% of the water TLC value and $\dot{V}_4 = 31.205$ l/s which is smaller than for water. Fig. 4 shows the QLC with IHE for MM in the T,s-diagram.

With decreasing T_5 the alkanes gain more interest and so cyclopentane, n-pentane, and isopentane are included in Table 5. They have an average value $\xi_P = 0.549 \pm 0.006$ with a maximum value of 0.555 for cyclopentane which is 95% of ξ_P for water. The volume flow

Table 6
Optimized results for case V ($T_5 = 423.15$ K, $T_7 = 288.15$ K, $T_1 = 311.15$ K, $T_u = 288.15$ K). All flow rates are given for a net power output $|\dot{W}|$ of 1 MW.

	Water[a]	Toluene	MM	Cyclopentane	n-Pentane	Isopentane	R245ca	Neopentane	n-Butane	Propane[a]
T_c (K)	647	592	520	512	470	461	448	434	425	370
IOS	–	0.112	0.331	0.059	0.114	0.108	0.082	0.109	0.050	–
Cycle type	TLC	TLC	TLC	TLC	TLC	TLC	TLC	TLC	TLC	ORCs2-
T_2 (K)	311.22	311.27	311.33	311.76	311.98	312.18	312.29	312.74	313.22	315.81
T_{2a} (K)	–	–	–	–	–	–	–	–	–	–
T_3 (K)	412	410	411	409	409	409	408	407	406	390
T_4 (K)	311.15	311.15	311.15	311.15	311.15	311.15	311.15	311.15	311.15	314.03
p_1 (kPa)	6.63	7.16	10.43	68.89	109.25	142.99	163.9	254.04	359.67	1309
p_3 (kPa)	350	203	268	905	1235	1455	1926	2069	2760	5097
$\dot{V}_3$ (l/s)	22.4	61.67	68.57	70.82	70.60	74.67	61.40	86.17	87.16	201.3
$\dot{V}_4$ (l/s)	69,896	74,256	52,508	10,378	7068	5708	4640	3662	2710	997
$\dot{m}_{WF}$ (kg/s)	20.73	46.27	42.96	43.23	34.17	35.11	61.71	35.57	33.82	27.34
$\dot{Q}_{2,2a}$ (MW)	–	–	–	–	–	–	–	–	–	–
x	0.16	0.41	0.81	0.46	0.66	0.68	0.67	0.79	0.71	Dry
η_{th}	0.114	0.115	0.115	0.112	0.111	0.111	0.109	0.108	0.107	0.102
T_6 (K)	321.22	323.24	323.22	324.06	323.65	324.51	323.58	325.09	326.06	335.48
T_p (K)	321	364	372	365	363	368	357	365	369	370
$\lvert\dot{Q}_{56}\rvert$ (MW)	8.80	8.73	8.73	8.92	9.02	9.04	9.15	9.25	9.38	9.77
$\dot{C}_{HC}$ (MW/K)	0.0863	0.0873	0.0873	0.0900	0.0907	0.0916	0.0918	0.0943	0.0966	0.111
T_8 (K)	301.15	301.15	301.15	301.15	301.15	301.15	301.15	301.15	301.15	301.42
$\dot{C}_{CA}$ (MW/K)	0.600	0.594	0.594	0.609	0.617	0.618	0.627	0.634	0.645	0.661
ξ	0.631	0.633	0.633	0.622	0.617	0.616	0.611	0.606	0.599	0.587
ξ_p	0.477	0.472	0.472	0.457	0.454	0.449	0.448	0.437	0.426	0.370

[a] Results are from [53].

rates $\dot{V}_4$ for the alkanes are also considerably smaller than those for water, the aromates, and the siloxanes. They increase from 3584 l/s for isopentane to 6429 l/s for cyclopentane with increasing T_c. Moreover, Fig. 2 shows the *T,s*-diagram for the cyclopentane TLC and Fig. 3 shows it for the n-pentane QLC without IHE. In addition, we consider also the refrigerant R245ca. It exhibits a TLC, has for the present case IV a rather low $\dot{V}_4$ but also the lowest ξ_P of the PCF shown in Table 5. We also want to mention that the maximum cycle temperatures T_3 of n-pentane, isopentane, and R245ca are close to their critical temperatures. For cyclopentane, however, T_3 is now 43 K lower than T_c. Hence, for case IV cyclopentane may be more interesting as working fluid for PFC than water.

Let us now compare the PFC-systems with the water CRC and the n-butane ORC. The water CRC shows again a small ξ_P and a slightly larger $\dot{V}_4$ than the water TLC. Considering the n-butane ORC it is seen that its ξ_P amounts to 88% to that of the water TLC and 92% to that of the cyclopentane TLC. On the other hand, the volume flow rate $\dot{V}_4$ of the n-butane ORC is the lowest in case IV.

5.5. Case V: $T_5 = 150$ °C, $T_7 = 15$ °C

Because of the trends in cases I to IV we present for case V in Table 6 PFC for water, toluene, MM, several alkanes, and R245ca and the ORC for propane. First, the Table shows that now all PFC-systems are of TLC type. Then we see that the water TLC has again the highest ξ_P amounting 0.477 which is followed closely by the ξ_P for toluene and MM. But for these three working fluids the volume flow rates $\dot{V}_4$ are rather high with the smallest value for MM which has the lowest T_c.

Next, we consider the TLC for the alkanes and R245ca. We see that the ξ_P values decrease from 0.457 for cyclopentane to 0.426 for n-butane and also that the $\dot{V}_4$ decrease from 10,378 l/s for cyclopentane to 2710 l/s for n-butane. As for cyclopentane ξ_P amounts to 96% of the water ξ_P and its $\dot{V}_4$ is only 15% of the value for water, cyclopentane may for case V again be a more interesting working fluid for PFC than water.

Considering finally the propane ORC it is seen that its ξ_P amounts to only 81% to that of the cylopentane TLC. On the other hand, the volume flow rate $\dot{V}_4$ for the ORC with propane is substantially lower than for all TLC-systems.

6. Summary and conclusions

Model results were presented for PFC-systems including the heat transfer to and from the cycles with aromates, siloxanes, and alkanes as working fluids. Five cases were studied which are characterized by different pairs of heat carrier and cooling agent inlet temperatures. The optimization criterion is the exergy efficiency for power production. Comparisons with previous results for water TLC and ORC as well as with new results for water CRC were made. For an assessment of the considered heat engines the most important quantities are the exergetic efficiency for power production ξ_P and the volume flow rate at the outlet of the expander $\dot{V}_4$ which determines the sizing of the system.

It was found that the TLC-systems with water have the highest or nearly highest power production efficiencies ξ_P among all systems considered. Whilst the volume flow rates $\dot{V}_4$ for water TLC are for the higher temperature intervals small to midsize, they become for the low temperature cases extremely large. For the low temperature cases IV and V we found that the TLC with cyclopentane are the best. It has a critical temperature T_c being only 79% of T_c of water and a very low IOS of 0.059. Whilst in cases IV and V the efficiencies ξ_P for the cyclopentane TLC amount to 95% and 96% of the water TLC values, the volume flow rates $\dot{V}_4$ for the cyclopentane TLC are only 15% of those for the water TLC.

For cases II and III the cyclopentane PFC gave also very good results for the efficiencies ξ_P and the volume flow rates $\dot{V}_4$. The problem with the optimized results presented here is the maximum cycle temperature $T_3 = 510$ K. This is rather close to the critical temperature of cyclopentane being $T_c = 512$ K which may cause problems in a real process. There are, however, indications that ξ_P as function of T_3 has a flat maximum which would allow to go to smaller values of T_3 without significant loss in efficiency.

Finally it is worth to mention that Smith [44] had also suggested to use in trilateral cycles mixtures as working fluids for which thermodynamic data can be calculated again with BACKONE [57,74]. Mixtures have the advantages that their critical temperature can be continuously varied with the composition and that the temperature glide during condensation better matches to the temperature profile of the cooling agent.

Acknowledgements

Ngoc Anh Lai, gratefully acknowledges financial support by the Vietnamese National Foundation for Science and Technology Development (NAFOSTED).

References

[1] Hammer H, Röhmfeld M. Abwärmenutzung zur Krafterzeugung mittels neuer Kreislaufmedien. In: VDI-Bericht, vol. 415. VDI-Verlag Düsseldorf; 1981. p. 81–7 [in German].
[2] ORC-HP-technology. In: VDI - Berichte 539. VDI–Verlag Düsseldorf, ISBN 3180905395; 1984. Proceedings of VDI-Seminar 10–12 Sept. 1984 ETH Zürich.
[3] Larjola J. Electricity from industrial heat using high-speed organic Rankine cycle (ORC). Int J Prod Econ 1995;41:227–35.
[4] Hung TC, Shai TY, Wang SK. A review of organic Rankine cycles (ORCs) for the recovery of low-grade waste heat. Energy 1997;22:661–7.
[5] Angelino G, Colonna P. Organic Rankine cycles for energy recovery from molten carbonate fuel cells. In: 35th intersociety energy conversion engineering conference and exhibit. Las Vegas, NV. Reston, VA: AIAA; 2000.
[6] Angelino G, Colonna P. Air cooled siloxane bottoming cycle for molten carbonate fuel cells. In: 2000 Fuel Cell Seminar, No 114, Portland, OR; 2000.
[7] Obernberger I, Hammerschmid A, Bini R. Biomasse-Kraft-Wärme-Kopplungen auf Basis des ORC-Prozesses-EU-THERMIE-Projekt Admont (A). In: Proc. VDI-Tagung "Thermische Nutzung von fester Biomasse", Salzburg, Mai 2001. VDI Bericht 1588. VDI-Verlag Düsseldorf, ISBN 3-18-091588-9; 2001. pp. 283–302 [in German].
[8] Saleh B, Koglbauer G, Wendland M, Fischer J. Working fluids for low-temperature organic Rankine cycles. Energy 2007;32:1210–21.
[9] Koglbauer G, Saleh B, Wendland M, Fischer J. Arbeitsmedien für Niedrigtemperatur-ORC-Prozesse, Proc. 9. Symposium Energieinnovation, 15–17. Februar 2006, TU Graz, Verlag der TU Graz, ISBN 3-902465-30-1, Graz 2006.pp 169 – 70. [in German].
[10] Hettiarachchia HDM, Golubovica M, Worek WM, Ikegami Y. Optimum design criteria for an organic Rankine cycle using low-temperature geothermal heat sources. Energy 2007;32:1698–706.
[11] Wei DH, Lu XS, Lu Z, Gu J. Performance analysis and optimization of organic Rankine cycle (ORC) for waste heat recovery. Energy Convers Manage 2007;48:1113–9.
[12] Drescher U, Brueggemann D. Fluid selection for the organic Rankine cycle (ORC) in biomass power and heat plants. Appl Therm Eng 2007;27:223–8.
[13] Desai NB, Bandyopadhyay S. Process integration of organic Rankine cycle. Energy 2009;34:1674–86.
[14] Schuster A, Karellas S, Kakaras E, Spliethoff H. Energetic and economic investigation of organic Rankine cycle applications. Appl Therm Eng 2009;29:1809–17.
[15] Kosmadakis G, Manolakos D, Kyritsis S, Papadakis G. Comparative thermodynamic study of refrigerants to select the best for use in the high-temperature stage of a two-stage organic Rankine cycle for RO desalination. Desalination 2009;243:74–94.
[16] Dai YP, Wang JF, Gao L. Parametric optimization and comparative study of organic Rankine cycle (ORC) for low grade waste heat recovery. Energy Convers Manage 2009;50:576–82.
[17] Wang XD, Zhao L. Analysis of zeotropic mixtures used in low-temperature solar Rankine cycles for power generation. Solar Energy 2009;83:605–13.
[18] Chacartegui R, Sanchez D, Munoz JM, Sanchez T. Alternative ORC bottoming cycles for combined cycle power plants. Appl Energy 2009;86:2162–70.
[19] Yari M. Exergetic analysis of various types of geothermal power plants. Renewable Energy 2010;35:112–21.
[20] Tchanche BF, Papadakis G, Lambrinos G, Frangoudakis A. Fluid selection for a low-temperature solar organic Rankine cycle. Appl Therm Eng 2009;29:2468–76.
[21] Lakew AA, Bolland O. Working fluids for low-temperature heat source. Appl Therm Eng 2010;30:1262–8.
[22] Lai NA, Wendland M, Fischer J. Working fluids for high-temperature organic Rankine cycles. Energy 2011;36:199–211.
[23] Gang Pei, Jing Li, Yunzhu Li, Dongyue Wang, Jie Ji. Construction and dynamic test of a small-scale organic Rankine cycle. Energy 2011;36:3215–23.
[24] Guo T, Wang HX, Zhang SJ. Fluids and parameters optimization for a novel cogeneration system driven by low temperature geothermal sources. Energy 2011;36:2639–49.
[25] Sauret E, Rowlands AS. Candidate radial-inflow turbines and high-density working fluids for geothermal power systems. Energy 2011;36:4460–7.
[26] Tchanche BF, Lambrinos G, Frangoudakis A, Papadakis G. Low-grade heat conversion into power using organic Rankine cycles – a review. Renewable Sustainable Energy Rev 2011;15:3963–79.
[27] Siddiqi MA, Atakan B. Investigation of the criteria for fluid selection in Rankine cycles for waste heat recovery. Int J Thermodyn 2011;14:117–23.
[28] Heberle F, Preißinger M, Brüggemann D. Zeotropic mixtures as working fluids in Organic Rankine Cycles for low-enthalpy geothermal resources. Renewable Energy 2012;37:364–70.
[29] DiPippo R. Second law assessment of binary plants generating power from low - temperature geothermal fluids. Geothermics 2004;33:565–86.
[30] Wang J, Dai Y, Gao L. Exergy analyses and parametric optimizations for different cogeneration power plants in cement industry. Appl Energy 2009;86:941–8.
[31] Bombarda P, Ivernizzi CM, Pietra C. Heat recovery from diesel engines: a thermodynamic comparison between Kalina and ORC cycles. Appl Therm Eng 2010;30:212–9.
[32] Kalina AI. Combined-cycle system with novel bottoming cycle. J Eng Gas Turbines Power – Trans ASME 1984;106:737–42.
[33] Wall G, Chuang CC, Ishida M. Exergy study of the Kalina cycle. In: Bajura RA, von Spakovsky MR, Geskin ES, editors. Analysis and design of energy systems: analysis of industrial processes, vol. 10-3; 1989. p. 73–7. Advanced Energy Systems, ASME, http://exergy.se/ftp/kalina.pdf; 1989.
[34] Park YM, Sonntag RE. A preliminary study of the Kalina power cycle in connection with a combined cycle system. Int J Energy Res 1990;14:153–62.
[35] Marston CH. Parametric analysis of the Kalina cycle. J Eng Gas Turbines Power – Trans ASME 1990;112:107–16.
[36] Heppenstall T. Advanced gas turbine cycles for power generation: a critical review. Appl Therm Eng 1998;18:837–46.
[37] Hettiarachchi HDM, Golubovic M, Worek WM, Ikegami Y. The performance of the Kalina cycle system 11 (KSC–11) with low-temperature heat sources. J Energy Resour Technol-Trans ASME 2007;129:243–7.
[38] Smith IK, Martin PR. Power from low-grade heat-sources – project sphere – an evaluation of the trilateral wet vapour cycle. Chartered Mech Eng 1985;32:30–3.
[39] Wilson SS. Trilateral cycles. Chartered Mech Eng 1985;32:11.
[40] Smith IK. Matching and work ratio in elementary thermal power plant theory. Proc Inst Mech Eng, Part A: J Power Energy 1992;206:257–62.
[41] Smith IK. Development of the trilateral flash cycle system. 1. Fundamental considerations. Proc Inst Mech Eng, Part A: J Power Energy 1993;207:179–94.
[42] Barclay FJ. Development of the trilateral flash cycle system. 1. Fundamental considerations. Proc Inst Mech Eng, Part A: J Power Energy 1994;208:153–4.
[43] Smith IK. Development of the trilateral flash cycle system. 1. Fundamental considerations - reply. Proc Inst Mech Eng, Part A: J Power Energy 1994;208:154.
[44] Smith IK, Dasilva RPM. Development of the trilateral flash cycle system. 2. Increasing power output with working fluid mixtures. Fundamental considerations. Proc Inst Mech Eng, Part A: J Power Energy 1994;208:135–44.
[45] Crook AW. Profiting from low-grade heat. The watt committee on energy report No. 26. Institution of Electrical Engineers; 1994. ISBN-10: 0852968353, ISBN-13: 978–0852968352.
[46] Smith IK, Stosic N, Aldis CA. Development of the trilateral flash cycle system. 3. The design of high-efficiency two-phase screw expanders. Proc Inst Mech Eng, Part A: J Power Energy 1996;210:75–93.
[47] Kliem BP. Grundlagen des Zweiphasen-Schraubenmotors - Fundamentals of the Two-Phase Screw-Type Engine, Dissertation, Fakultät für Maschinenbau, Universität Dortmund, 2005 [in German].
[48] Löffler M. Kreisprozess mit Flashverdampfung im Arbeitsraum einer Kolbenmaschine. VGB PowerTech. Int J Electricity Heat Generation 2007;7:92–7 [in German].
[49] DiPippo R. Ideal thermal efficiency for geothermal binary plants. Geothermics 2007;36:276–85.
[50] Löffler M. Flash evaporation in cyclones. Chem Eng Technol 2008;31:1062–5.
[51] Zamfirescu C, Dincer I. Thermodynamic analysis of a novel ammonia–water trilateral Rankine cycle. Thermochimica Acta 2008;447:7–15.
[52] Löffler M, Steffen M, Schaber K. Umsetzung einer Kolbendampfmaschine mit interner Flashverdampfung, Abschlussbericht über ein Entwicklungsprojekt, gefördert unter dem Az: 25116 – 21/0. von der Deutschen Bundesstiftung Umwelt (DBU) [in German], http://www.dbu.de/phpTemplates/publikationen/pdf/040412020045cg4k.pdf; 2010.
[53] Fischer J. Comparison of trilateral cycles and organic Rankine cycles. Energy 2011;36:6208–19.
[54] Clausius R. Über die Anwendung der mechanischen Wärmetheorie auf die Dampfmaschine. Ann Phys Chem 1854;173:441–76. 513–558 [in German].
[55] Rankine WJM. Miscellaneous scientific papers. London: Charles Griffin and Company, http://www.archive.org/details/miscellaneoussci00rank; 1881.
[56] Tabor H, Bronicki L. Establishing criteria for fluids for small vapour turbines. SAE Trans 1965;73:561–75.
[57] Wendland M, Saleh B, Fischer J. Accurate thermodynamic properties from the BACKONE equation for the processing of natural gas. Energy Fuels 2004;18:938–51.
[58] Saleh B, Wendland M. Screening of pure fluids as alternative refrigerants. Int J Refrig 2006;29:260–9.
[59] Lai NA, Wendland M, Fischer J. Description of linear siloxanes with PC-SAFT equation. Fluid Phase Equilibria 2009;283:22–30.
[60] Chen SS, Wilhoit RC, Zwolinski BJ. Ideal gas thermodynamic properties and isomerization of n-butane and isobutene. J Phys Chem Ref Data 1975;4:859–69.
[61] Prausnitz JM, Poling BE, O'Connell JP. The properties of gases and liquids. 5th ed. New York: McGraw-Hill; 2001.
[62] Gillis KA. Thermodynamic properties of seven gaseous halogenated hydro-hydrocarbons from acoustic measurements: CHClFCF3, CHF2CF3, CF3CH3, CHF2CH3, CF3CHFCHF2, CF3CH2CF3, and CHF2CF2CH2F. Int J Thermophysics 1997;18:73–135.

[63] Pitzer KS, Kilpatrick JE. The entropies and related properties of branched paraffin hydrocarbons. Chem Rev 1946;39:435–47.
[64] Dorofeeva OV, Gurvich LV, Jorish VS. Thermodynamic properties of twenty-one monocyclic hydrocarbons. J Phys Chem Ref Data 1986;15:437–64.
[65] Nannan NR, Colonna P, Tracy CM, Rowley RL, Hurly JJ. Ideal-gas heat capacities of dimethylsiloxanes from speed-of-sound measurements and ab initio calculations. Fluid Phase Equilibria 2007;257:102–13.
[66] Pitzer KS, Scott DW. The thermodynamics and molecular structure of benzene and its methyl derivatives. J Am Chem Soc 1943;65:803–29.
[67] Miller A, Scott DW. Chemical thermodynamic properties of ethylbenzene. J Chem Phys 1978;68:787–1324.
[68] Abbas R, Schedemann A, Ihmels C, Enders S, Gmehling J. Measurement of thermophysical pure component properties for a few siloxanes used as working fluids for organic Rankine cycles. Ind Eng Chem Res 2011;50: 9748–57.
[69] NIST Chemistry WebBook, Thermophysical properties of fluids, http://webbook.nist.gov/chemistry/fluid/.
[70] Huber ML, Ely JF. A predictive extended corresponding states model for pure and mixed refrigerants including an equation of state for R134a. Int J Refrig 1994;17:18–31.
[71] Polt A, Platzer B, Maurer G. Parameter der thermischen Zustandsgleichung von Bender fuer 14 mehratomige reine Stoffe. Chem Tech (Leipzig) 1992;44: 216–24 [in German].
[72] Müller A, Winkelmann J, Fischer J. The backbone family of equations of state: 1. Nonpolar and polar pure fluids. AIChE J 1996;42:1116–26.
[73] Wagner W, Pruss A. The IAPWS formulation 1995 for the thermodynamic properties of ordinary water substance for general and scientific use. J Phys Chem Ref Data 2002;31:387–535.
[74] Weingerl U, Wendland M, Fischer J, Müller A, Winkelmann J. Backone family of equations of state: 2. Nonpolar and polar fluid mixtures. AIChE J 2001;47:705–17.